Surface reconstruction of pure-Cu single-crystal electrodes under Co-reduction potentials in alkaline solutions: A study by seriatim ECSTM-DEMS

Youn-Geun Kim, Alnald Javier, Jack H. Baricuatro, Daniel Torelli, Kyle D. Cummins, Chu F. Tsang, John C. Hemminger, Manuel P. Soriaga

PII: S1572-6657(16)30486-6
DOI: doi: 10.1016/j.jelechem.2016.09.029
Reference: JEAC 2843

To appear in: *Journal of Electroanalytical Chemistry*

Received date: 31 July 2016
Revised date: 17 September 2016
Accepted date: 20 September 2016

Please cite this article as: Youn-Geun Kim, Alnald Javier, Jack H. Baricuatro, Daniel Torelli, Kyle D. Cummins, Chu F. Tsang, John C. Hemminger, Manuel P. Soriaga, Surface reconstruction of pure-Cu single-crystal electrodes under Co-reduction potentials in alkaline solutions: A study by seriatim ECSTM-DEMS, *Journal of Electroanalytical Chemistry* (2016), doi: 10.1016/j.jelechem.2016.09.029

J. Electroanal. Chem.
Short Communication
Revised September 2016

SURFACE RECONSTRUCTION OF PURE-CU SINGLE-CRYSTAL ELECTRODES UNDER CO-REDUCTION POTENTIALS IN ALKALINE SOLUTIONS: A STUDY BY *SERIATIM* ECSTM-DEMS

Youn-Geun Kim, Alnald Javier, Jack H. Baricuatro, Daniel Torelli,

Kyle D. Cummins, Chu F. Tsang, John C. Hemminger and Manuel P. Soriaga[1]

Joint Center for Artificial Photosynthesis

California Institute of Technology

Pasadena, CA 91125

[1]Corresponding author. Email Address: msoriaga@caltech.edu

ABSTRACT

Quasi-operando electrochemical scanning tunneling microscopy (ECSTM) recently showed that a polycrystalline Cu electrode kept in 0.1 *M* KOH at -0.9 V (SHE), a potential very close to that for electrochemical CO reduction, underwent a two-step surface reconstruction, initially to Cu(111), or Cu(pc)-[Cu(111)], and terminally to Cu(100), or Cu(pc)-[Cu(100)]. When subjected to monolayer-limited $Cu_{(s)} \leftrightarrow Cu_2O_{(s)}$ oxidation-reduction cycles (ORC), the Cu(pc)-[Cu(100)] surface was further transformed to Cu(pc)-[Cu(511)] that produced C_2H_5OH exclusively, as detected by differential electrochemical mass spectrometry, at an overvoltage lower by 645 mV relative to that for the formation of hydrocarbons. In this paper, results are presented from studies with the native monocrystalline surfaces Cu(111), Cu(100) and Cu(110). Whereas the intermediate Cu(pc)-[Cu(111)] layer was eventually converted to Cu(pc)-[Cu(100)], the surface of a pristine Cu(111) single crystal itself showed no such conversion. The surface of an original Cu(100) electrode likewise proved impervious to potential perturbations. In contrast, the outer plane of a Cu(110) crystal underwent three transformations: first to disordered Cu(110)-*d*[Cu(110)], then to disordered Cu(110)-*d*[Cu(111)], and finally to an ordered Cu(110)-[Cu(100)] plane. After multiple ORC, the converted [Cu(100)] lattice atop the Cu(110) crystal did not generate ethanol, in contrast to the [Cu(100)] phase above the Cu(pc) bulk. *Quasi-operando* ECSTM captured the disparity: Post-ORC, Cu(110)-[Cu(100)] was converted, not to Cu(110)-[Cu(511)], but to an ordered but catalytically inactive Cu(110)-[Cu(111)]; hence, no C_2H_5OH production upon reduction of CO, as would have been the case for a stepped Cu(511) surface.

KEYWORDS

Surface Reconstruction of Cu Electrodes Under CO-reduction Potentials
Quasi-operando Electrochemical Scanning Tunneling Microscopy
Differential Electrochemical Mass Spectrometry
Seriatim ECSTM-DEMS

INTRODUCTION

The influence of atomic-level surface structure on the reduction of CO at pure Cu electrodes has been investigated in the past [1-6] but those undertaken in alkaline solutions most likely will have to be re-examined because none of the studies, except for one [6], monitored the Cu surface under *operando* (or close to *operando*) potentials. In virtually all instances, surface structural information was acquired only before electrolysis, but none in the course of the reaction. In a few occasions, *ex situ* post-catalysis examinations were also carried out [7]. The single exception [6] involved a *quasi-operando* technique that combined electrochemical scanning tunneling microscopy (ECSTM) [8] and differential electrochemical mass spectrometry (DEMS) [9]. [1]

Seriatim or sequential ECSTM-DEMS is able to identify the particular surface structure that gives rise to a specific product selectivity because: (i) the volatile-product distribution of an electrocatalytic reaction can be analyzed by DEMS, and (ii) proximate to the potential of the reaction, the structure of the (well-ordered) surface can be observed by ECSTM. The consolidated ECSTM-DEMS technique, however, cannot be carried out in true *operando* fashion since, at optimum reduction potentials, the catalytic activities (faradaic current densities) are too high, and the resulting interferences with the tunneling currents seriously degrade the quality of the ECSTM images; in addition, ECSTM and DEMS are conducted separately in their own discrete compartments although with complementary experimental set-ups that guarantee identical electrochemical pretreatment and catalysis conditions. The use of *quasi-operando* as a descriptor thus appears more appropriate.

Our *seriatim* ECSTM-DEMS work investigated the preferential reduction of CO to C_2H_5OH on Cu in 0.1 *M* KOH at -1.06 V; this value represents an overpotential of only 485 mV

[1] It may be mentioned that *in situ* wide-scale morphological and zoomed-in atom-resolved STM images in acid solutions have been reported for Cu overlayers supported on Pt or Au single-crystal substrates [10,11]; hence, the samples were not categorized as pure Cu.

relative to the standard CO-to-C_2H_5OH reduction potential [12], and lower by 645 mV than for the production of hydrocarbons like CH_4 or C_2H_4 [13, 14]. We observed that an atomically ordered Cu(100) surface did not produce ethanol. However, when a polycrystalline Cu electrode was kept at -0.9 V in 0.1 *M* KOH, the surface underwent reconstruction, first to Cu(111), designated as Cu(pc)-[Cu(111)], and then to Cu(100), represented as Cu(pc)-[Cu(100)]. When the latter was subjected to mild (monolayer-limited) $Cu \leftrightarrow Cu_2O$ cycles, further transformation resulted in an ordered stepped surface, Cu(S)-[3(100)×(111)], or Cu(511), that engendered the selective production of ethanol.

The potential-driven surface reconstruction and the sequential ECSTM-DEMS experiments above have been extended to the native monocrystalline surfaces Cu(111), Cu(100) and Cu(110). The results are the subject of the present *Short Communication*.

EXPERIMENTAL

The experimental procedures adopted in this study have been described in better detail elsewhere [6] and will only be summarized here.

A BioLogic SP-300 potentiostat (BioLogic Science Instruments, Claix, France) equipped for electrochemical impedance spectroscopy (EIS) to determine the uncompensated solution resistance was used for the DEMS experiments. The ECSTM potentiostat was part of the STM system, an Agilent 5500 microscope (Agilent Technologies, Santa Clara, CA) or a Nanoscope E microscope (Digital Instruments, Santa Barbara, CA). All solutions were prepared using an 18.2 MΩ-cm Nanopure water (ThermoFisher Scientific, Asheville, NC). Potentials are referenced to the standard hydrogen electrode (E_{SHE}) since it is directly relatable to thermodynamic free-energy changes and do not mask pH effects; $E_{SHE} = E_{RHE} - 0.059$ pH.

The STM electrochemical cell, custom-crafted from Kel-F (Emco Industrial Plastics, Inc., Cedar Grove, NJ), was fitted with a Pt counter electrode and a pre-calibrated Pt pseudo-reference electrode [15]. The STM tips were prepared by an electrochemical etch of a 0.25 mm diameter tungsten wire (Sigma-Aldrich, St. Louis, MO) in 0.6 *M* KOH at 15 VAC. All images were acquired after one-hour polarization at -0.9 V; a high-resolution scanner was employed in constant-current mode without post-scan operations. The Cu electrodes were commercially oriented 1.0-mm-thick Cu(100), Cu(110) and Cu(111) single crystals, 10 mm in diameter and 99.999% in purity (Princeton Scientific Corp., Easton, PA). Prior to use, the disk electrode was metallographically polished to a mirror finish with a suspension of polycrystalline diamond (Buehler, Lake Bluff, IL) at a grain size of 0.05 μm. The disk was electropolished in 85% H_3PO_4 (Sigma-Aldrich) at 2.0 V for 10 s with a Pt counter electrode; it was then ultrasonicated in, and later rinsed with, deaerated Nanopure water. The polished sample was not thermally annealed. The alkaline solution, 0.1 *M* KOH, used in this study was prepared from analytical-grade KOH (Sigma-Aldrich) and was purged for at least 1 h in oxygen-free, ultrahigh purity argon (Airgas, Radnor, PA). These same electrodes were used for the DEMS experiments.

The discretely prepared Cu electrodes were then transferred with a protective layer of electrolyte to the DEMS cell fabricated out of polyether ether ketone. A 20-μm-thick polydimethylsiloxane (PDMS) membrane with 20-nm porosity isolated the electrochemical cell from the mass spectrometry compartment, and a 50-μm glass spacer separated the Cu electrode from the PDMS membrane that resulted in a thin-layer electrochemical cell with a volume of 5.0 μL. A porous glass frit placed between the Cu cathode and Pt anode electrodes precluded the oxidation of the CO-reduction products. The potential of the Cu electrode was held at -1.06 V for 600 s while the reduction products were monitored by an HPR-20 quadrupole mass spectrometer (Hiden Analytical, Warrington, England) with a secondary-electron-multiplier detector at a voltage of 950 V and an emission current of 50 μA. It will be recalled that, in DEMS, only species that are hydrophobic and/or volatile can be readily monitored. At least three separate trials were performed for ECSTM; two for DEMS.[2]

In some instances, the ordered electrodes were subjected to mild (monolayer-limited) oxidation-reduction cycles (ORC) via multiple voltammetric scans, at 50 mV s^{-1}, between 0.1 V and -0.9 V. The intent was to induce minimal surface transformations and determine what their influences are on the product distribution. At 0.1 V, a single layer of copper(I) oxide, was formed; at -0.9 V, the surface oxide was reduced back to Cu [8]. Within this potential window, any structural transformations remained discernible by ECSTM. In contrast, excursions to more positive potentials yield multilayers of copper(II) oxide that, upon reduction, led to extensive surface roughness which then precluded ECSTM experiments [16].

[2] The DEMS procedure employed in this study is quantitative since the absolute quantities of products are determined by calibration, as previously described [17]. For example, the concentration of ethanol, the lone CO-reduction product, can be extracted from a plot of its ion current as a function of the concentration of reference solutions. When that amount of alcohol is used in Faraday's Law, the electrolytic charge for only the CO-to-CH_3CH_2OH reduction can be calculated. The ratio of such charge to the total charge, measured for the duration of the constant-potential electrolysis, yields the current or Faradaic efficiency of the ethanol-production reaction. The external calibration also indicated that the lowest detectable concentration of ethanol is 500 μM.

RESULTS AND DISCUSSION

Figure 1 shows *operando* ECSTM images [3] that illustrate the instability of a polycrystalline Cu electrode surface, denoted by Cu(pc), when it is held in 0.1 *M* KOH at -0.9 V (SHE), a potential in close proximity to that often adopted in the electrochemical reduction of CO in alkaline solution. Sub-micrometer-sized islands are discernible, but the atomic arrangements could not be imaged because of excessive roughness. After 15 minutes, the surface started to show signs of a reconstruction, completed after a total of 30 minutes, to a distinctive array of triangular domains. The terrace atoms were of hexagonal rotational symmetry, indicative of a Cu(111) surface, as resolved by the high-resolution (2 nm x 2 nm) imagery posted as an inset in Figure 1. After 15 additional minutes, or an aggregate of 45 minutes, a second surface transformation took place, as can be seen by the emergence of rectangular patches alongside the Cu(111) domains. In less than 60 minutes, the second reconstruction was completed, as evidenced by the presence of only rectangular domains. High-resolution interrogation of the terraces revealed a square lattice with an interatomic distance of 0.27 ± 0.01 nm, a value that closely matches that for a pristine, oxide-free Cu(100) lattice [18]. The two-step reconstruction may be represented in equation form as [16]:

$$\text{Cu(pc)} \rightarrow \text{Cu(pc)-[Cu(111)]} \quad (1)$$

$$\text{Cu(pc)-[Cu(111)]} \rightarrow \text{Cu(pc)-[Cu(100)]} \quad (2)$$

In the equations, the square-bracketed notation [Cu(*hkl*)] identifies the reconstructed overlayer. It is without dispute that, unlike high-temperature surface reconstruction, the potential-induced transformation at ambient temperature is limited to only a few surface layers. However, it is not known at this time how many layers are involved.

[3] It cannot be overemphasized that, whereas the ECSTM images displayed in this paper are only for nanometer-scale domains on the bulk crystal, those are representative of the entire surface because numerous images have been evaluated throughout the macroscopic surface. The default protocol, in this and other STM studies, has always been that results will be adopted only if satisfactory agreement exists among all the sampled images [6].

Figure 2 displays *operando* ECSTM images for the pristine single crystals Cu(111) and Cu(100) subjected to the same conditions as Cu(pc) in Figure 1. In contrast to Cu(pc), the native Cu(111) and Cu(100) surfaces exhibited remarkable stability up to four hours; longer times were not investigated. While the stability of Cu(100) at -0.9 V in 0.1 *M* KOH is not unexpected in view of the results depicted in Figure 1, the inertness of the native Cu(111) surface is a quandary because, as indicated in Figure 1, the reconstructed Cu(pc)-[Cu(111)] eventually transforms to Cu(pc)-[Cu(100)]. The reason for the non-reconstruction is not fully understood, but it may have its origin in the comparative adhesions of various surfaces in contact with one another. For example, the adhesion coefficient of a Cu(100) plane in contact another Cu(100) surface is five times larger than that for a Cu(111) surface in contact with a Cu(100) plane [19].

Cu(110) is actually a stepped surface that consists of a terrace row of (111) atoms and a monoatomic step also of (111) atoms. The expectation is for the plane to be more stable than Cu(pc), but the absence of wide planar terraces may render it less stable than the Cu(111) and Cu(100) faces. This expectation appears to be borne out by the data in Figure 3. The topmost layer(s) of the Cu(110) crystal underwent three comparatively facile reconstructions: The first was to a disordered Cu(110)-*d*[Cu(110)], where *d* denotes a disordered reconstructed layer. The second was to a disordered Cu(110)-*d*[Cu(111)], and the third step to an ordered Cu(110)-[Cu(100)] plane. In equation forms:

$$\text{Cu(110)} \rightarrow \text{Cu(110)-}d\text{[Cu(110)]} \quad (3)$$

$$\text{Cu(110)-}d\text{[Cu(110)]} \rightarrow \text{Cu(110)-}d\text{[Cu(111)]} \quad (4)$$

$$\text{Cu(110)-}d\text{[Cu(111)]} \rightarrow \text{Cu(110)-[Cu(100)]} \quad (5)$$

It is of interest to note that the final state in Equation (5) has a similarity with Equation (2) in that the topmost or reconstructed layer is a [Cu(100) face]. As recounted above, when that surface is subjected to multiple cycles of mild $Cu_{(s)} \leftrightarrow Cu_2O_{(s)}$ ORC, it is converted to another structure, a stepped [Cu(511)] overlayer, that spawns the exclusive production of ethanol upon

electrochemical reduction of CO. It was thus important to ascertain whether or not the two reconstructed [Cu(100)] structures both yielded C_2H_5OH after several ORC.

The results, in terms of post-ORC DEMS spectra for methane, ethylene and ethanol, are shown in Figure 4. None of the three organic products were produced at the Cu(110)-[Cu(100)] surface; in contrast, the Cu(pc)-[Cu(100)] electrode generated ethanol exclusively [6]. This can only mean that, despite the fact that the reconstructed layers are structurally identical, the transformations brought about by the multiple $Cu_{(s)} \leftrightarrow Cu_2O_{(s)}$ cycles differed for the two adlattices; it was obvious that a [Cu(511)] structure was not generated from the Cu(110)-[Cu(100)] surface since no ethanol was produced. The high-resolution ECSTM images shown in Figure 5 indeed provides evidence for the disparate outcomes: The totally unexpected result was that the Cu(110)-[Cu(100)] was reorganized back to Cu(110)-[Cu(111)] but with the overlayer now in a highly ordered arrangement; it is not understood why this unforeseen reconstruction-reversal transpired. Figure 6 displays DEMS spectra for pristine Cu(100) and Cu(111), confirmation that a pristine Cu(111) surface is inert towards CO-to-C_2H_5OH reduction under conditions of low overpotential in alkaline solution. Evidently, the ORC-reconstructed but ordered [Cu(111)] atop the bulk Cu(110) base behaves similarly to a native Cu(111) surface.

CONCLUSIONS

The atomic-level structural stability and ethanol-product-selectivity of pristine Cu(111), Cu(100) and Cu(110) single-crystalline surfaces were investigated under low-overpotential CO-reduction conditions, -0.9 V in 0.1 *M* KOH, by combined *quasi-operando* electrochemical scanning tunneling microscopy and differential electrochemical mass spectrometry, to compare their behavior with that of polycrystalline Cu(pc). The most noteworthy observations: (i) Whereas the reconstructed [Cu(111)] layer atop the Cu(pc) bulk was eventually converted to [Cu(100)], the surface of a native Cu(111) electrode itself showed no such conversion. (ii) The surface of an original Cu(100) electrode likewise proved impervious to potential perturbations. (iii) In a different outcome, the topmost planes of a Cu(110) crystal underwent three transformations: first to disordered Cu(110)-*d*[Cu(110)], then to disordered Cu(110)-*d*[Cu(111)], and finally to an ordered Cu(110)-[Cu(100)] plane. (iv) After multiple monolayer-limited Cu-to-Cu_2O oxidation-reduction cycles, the converted [Cu(100)] lattice atop the Cu(110) crystal was inert with respect to selective production of ethanol, in contrast to the [Cu(100)] phase above the Cu(pc) bulk. (v) *Quasi-operando* ECSTM showed that, after several ORC, the Cu(110)-[Cu(100)] adlattice was not converted to Cu(110)-[Cu(511)], but to a well-ordered but catalytically inactive Cu(110)-[Cu(111)] layer; hence, there was no C_2H_5OH production upon reduction of CO, as would have been the case for a stepped Cu(511) surface.

ACKNOWLEDGMENTS

This material is based upon work performed by the Joint Center for Artificial Photosynthesis, a DOE Energy Innovation Hub, supported through the Office of Science of the U.S. Department of Energy under Award No. DE-SC0004993.

REFERENCES

[1] Y. Hori, R. Takahashi, Y. Yoshinami, A. Murata, Electrochemical Reduction of CO at a Copper Electrode, J. Phys. Chem. B 101 (1997) 7075-7081.

[2] Y. Hori, A. Murata, R. Takahashi, S. Suzuki, Electroreduction of Carbon Monoxide to Methane and Ethylene at a Copper Electrode in Aqueous Solutions at Ambient Temperature and Pressure, J. Am. Chem. Soc. 109 (1987) 5022-5023

[3] Y. Hori, I. Takahashi, O. Koga, N. Hoshi, N. Selective Formation of C2 Compounds From Electrochemical Reduction of CO_2 at a Series of Copper Single Crystal Electrodes, J. Phys. Chem. B 106 (2002) 15-17.

[4] K.J.P. Schouten, Z. Qin, E.P. Gallent, M.T.M. Koper, Two Pathways for the Formation of Ethylene in CO Reduction on Single-crystal Copper Electrodes, J. Am. Chem. Soc. 134 (2012) 9864-9867.

[5] F. Calle-Vallejo, M.T.M. Koper, Theoretical Considerations on the Electroreduction of CO to C_2 Species on Cu(100) Electrodes. Angew. Chem. Int. Ed. 52 (2013) 7282-7285.

[6] Y.-G. Kim, A. Javier, J.H. Baricuatro, M.P. Soriaga, Regulating the Product Distribution of CO Reduction by the Atomic-level Structural Modification of the Cu Electrode Surface, Electrocatalysis. DOI 10.1007/s12678-016-0314-1 (2016).

[7] A. Verdaguer-Casadevall, C.W. Li, T.P. Johansson, S.B. Scott, J.T. McKeown, M. Kumar, I.E.L. Stephens, M.W. Kanan, I. Chorkendorff, Probing the Active Surface Sites for CO Reduction on Oxide-derived Copper Electrocatalysts, J. Am. Chem. Soc. 137 (2015) 9808-9811.

[8] Y.-G. Kim, M.P. Soriaga, Cathodic Regeneration of a Clean and Ordered Cu(100)-(1×1) Surface from an Air-oxidized and Disordered Electrode: An Operando STM Study, J. Electroanal. Chem. 734 (2014) 7-9.

[9] A. Javier, B. Chmielowiec, J. Sanabria-Chinchilla, Y.-G. Kim, J.H. Baricuatro, M.P.

Soriaga, A DEMS Study of the Reduction of CO2, CO, and HCHO Pre-adsorbed on Cu Electrodes: Empirical Inferences on the CO2RR Mechanism, Electrocatalysis 6 (2015) 127-131.

[10] A. S. Varela, C. Schlaup, Z. P. Jovanov, P. Malacrida, S. Horch, I. E. L. Stephens and I. Chorkendorff, CO2 Electroreduction on Well-Defined Bimetallic Surfaces: Cu Overlayers on Pt(111) and Pt(211), J. Phys. Chem. C 117 (2013), 20500−20508.

[11] C. Schlaup, S. Horch, I. Chorkendorff, On the stability of copper overlayers on Au(111) and Au(100) electrodes under low potential conditions and in the presence on CO and CO2, Surface Science 631 (2015) 155–164

[12] C. W. Li, J. Ciston, M. W. Kanan, Electroreduction of Carbon Monoxide to Liquid Fuel on Oxide-derived Nanocrystalline Copper, Nature 508 (2014) 504-507.

[13] Y. Hori, Electrochemical CO2 Reduction on Metal Electrodes, in Modern Aspects of Electrochemistry, ed. by C.G. Vayenas, R.E. White, M.E. Gamboa-Aldeco (Springer, New York, 2008), p. 89.

[14] K.P. Kuhl, E.R. Cave, D.N. Abram, T.F. Jaramillo, New Insights into the Electrochemical Reduction of Carbon Dioxide on Metallic Copper Surfaces, Energy Environ. Sci. 5 (2012) 7050-7059.

[15] K. Itaya, In Situ Scanning Tunneling Microscopy in Electrolyte Solutions, Prog. Surf. Sci. 58 (1998) 121-247.

[16] Y.-G. Kim, J.H. Baricuatro, A. Javier, J.M. Gregoire, M.P. Soriaga, The Evolution of the Polycrystalline Copper Surface, First to Cu(111) and then to Cu(100), at a Fixed CO2RR Potential: A Study by Operando EC-STM, Langmuir 30 (2014) 15053-15056.

[17] A. Javier, J.H. Baricuatro, Y.-G. Kim and M.P. Soriaga, Overlayer Au-on-W Near-Surface Alloy for the Selective Electrochemical Reduction of CO2 to Methanol: Empirical (DEMS) Corroboration of a Computational (DFT) Prediction, Electrocatalysis 6 (2015) 493-497.

[18] R.E. Smallman, R.J. Bishop, Modern Physical Metallurgy and Materials Engineering, 6th

edn., Elsevier, Oxford, 1999, p 20.

[19] D.H. Buckley, Surface Effects in Adhesion, Friction, Wear, and Lubrication, Elsevier, Amsterdam, 1981, p 270.

Figure Captions

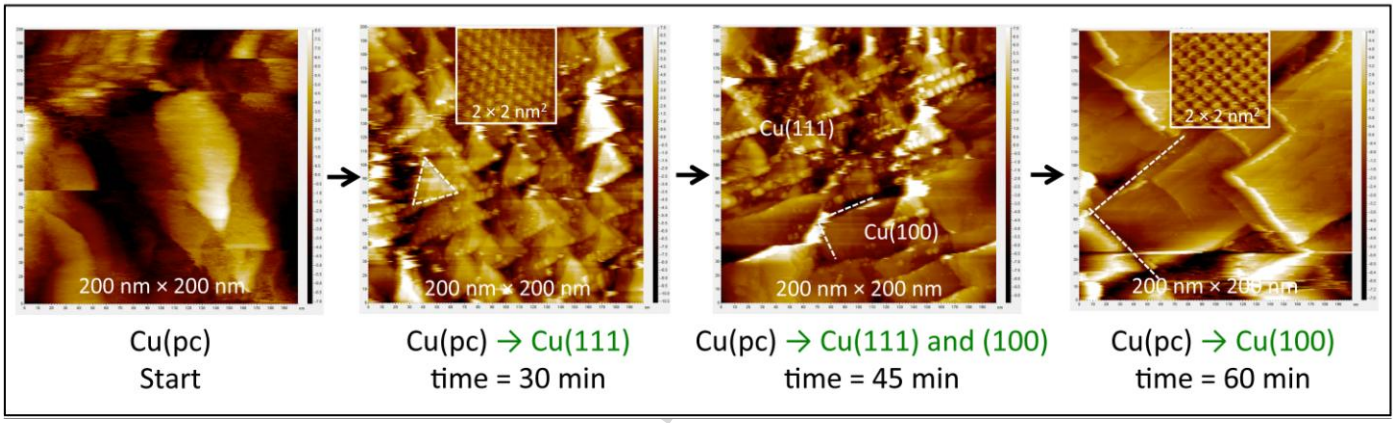

Figure 1. *Operando* electrochemical scanning tunneling microscopy (ECSTM) of a polycrystalline copper electrode, Cu(pc), held at -0.9 V in 0.1 *M* KOH for preselected times of 0, 30, 45 and 60 minutes. Bias voltage = 250 mV; tunneling current, 2 nA. Other experimental details are as indicated in the text.

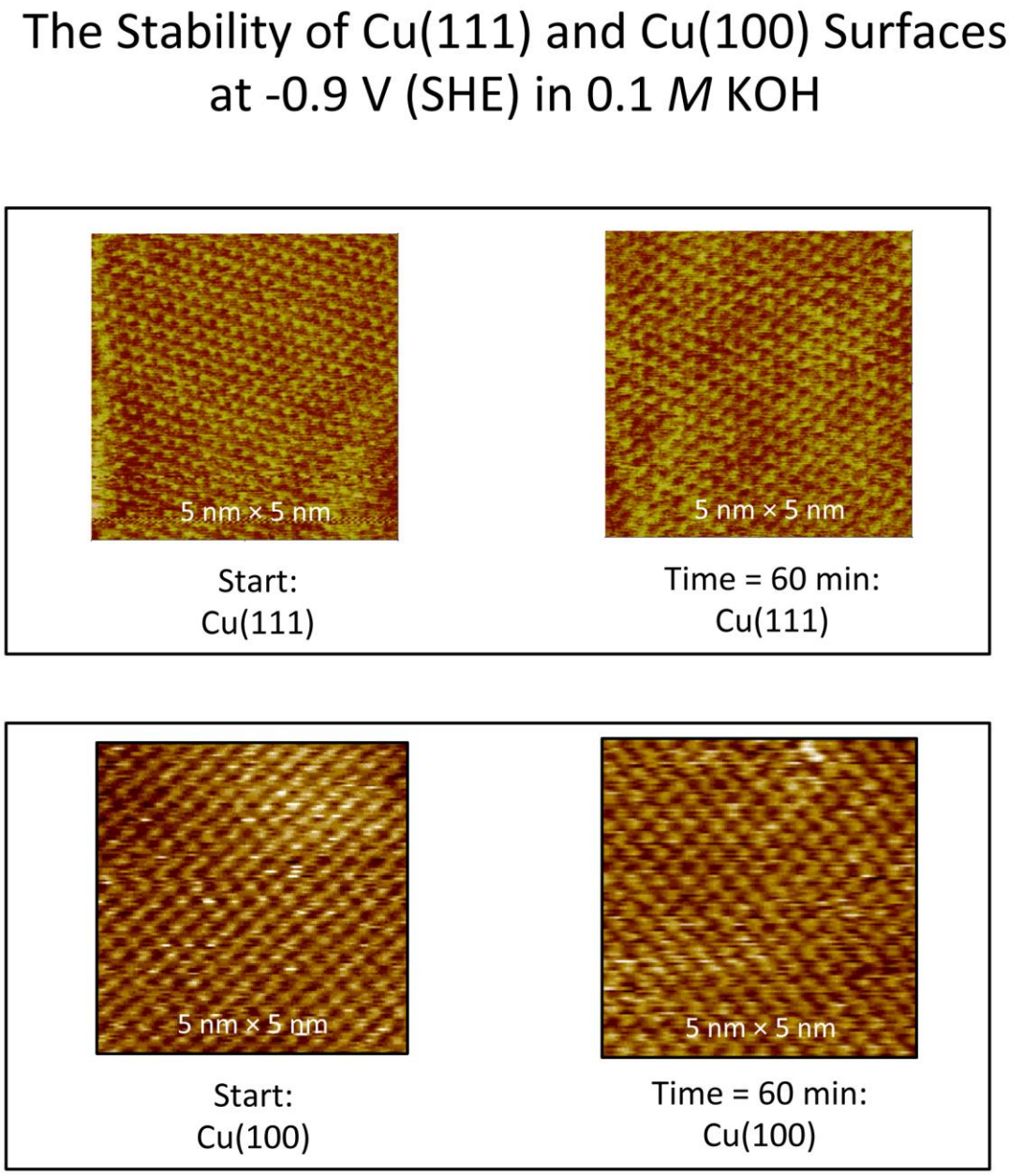

Figure 2. *Operando* electrochemical scanning tunneling microscopy (ECSTM) of pristine Cu(111) and Cu(100) electrodes held at -0.9 V in 0.1 *M* KOH for 0 and 60 minutes. Experimental conditions were as in Figure 1.

The Stability of the Cu(110) Surface at -0.9 V (SHE) in 0.1 *M* KOH

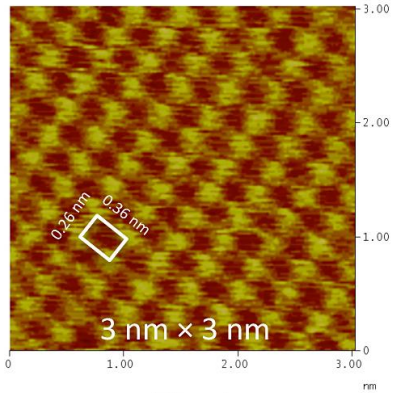

Start:
Cu(110)

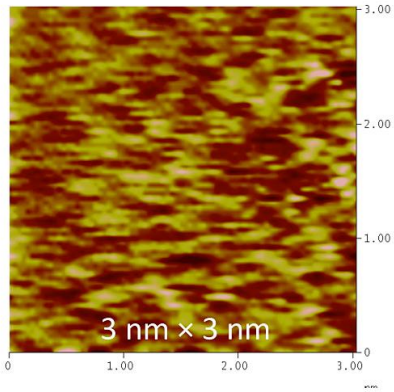

Time = 20 min:
Disordered Cu(110)

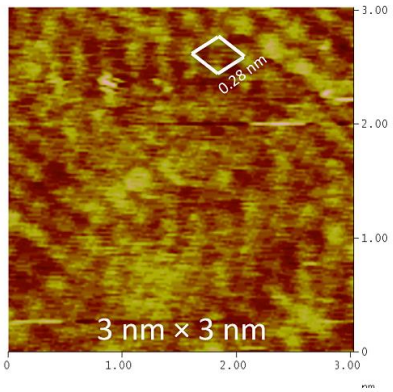

Time = 40 min:
Disordered Cu(111)

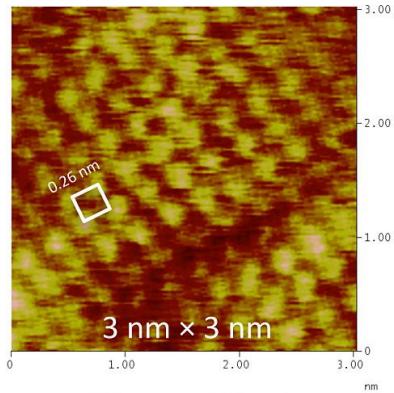

Time = 60 min:
Cu(100)

Figure 3. *Operando* electrochemical scanning tunneling microscopy (ECSTM) of a native Cu(110) electrode held at -0.9 V in 0.1 *M* KOH, at 0 and 60 minutes. Experimental conditions were as in Figure 1.

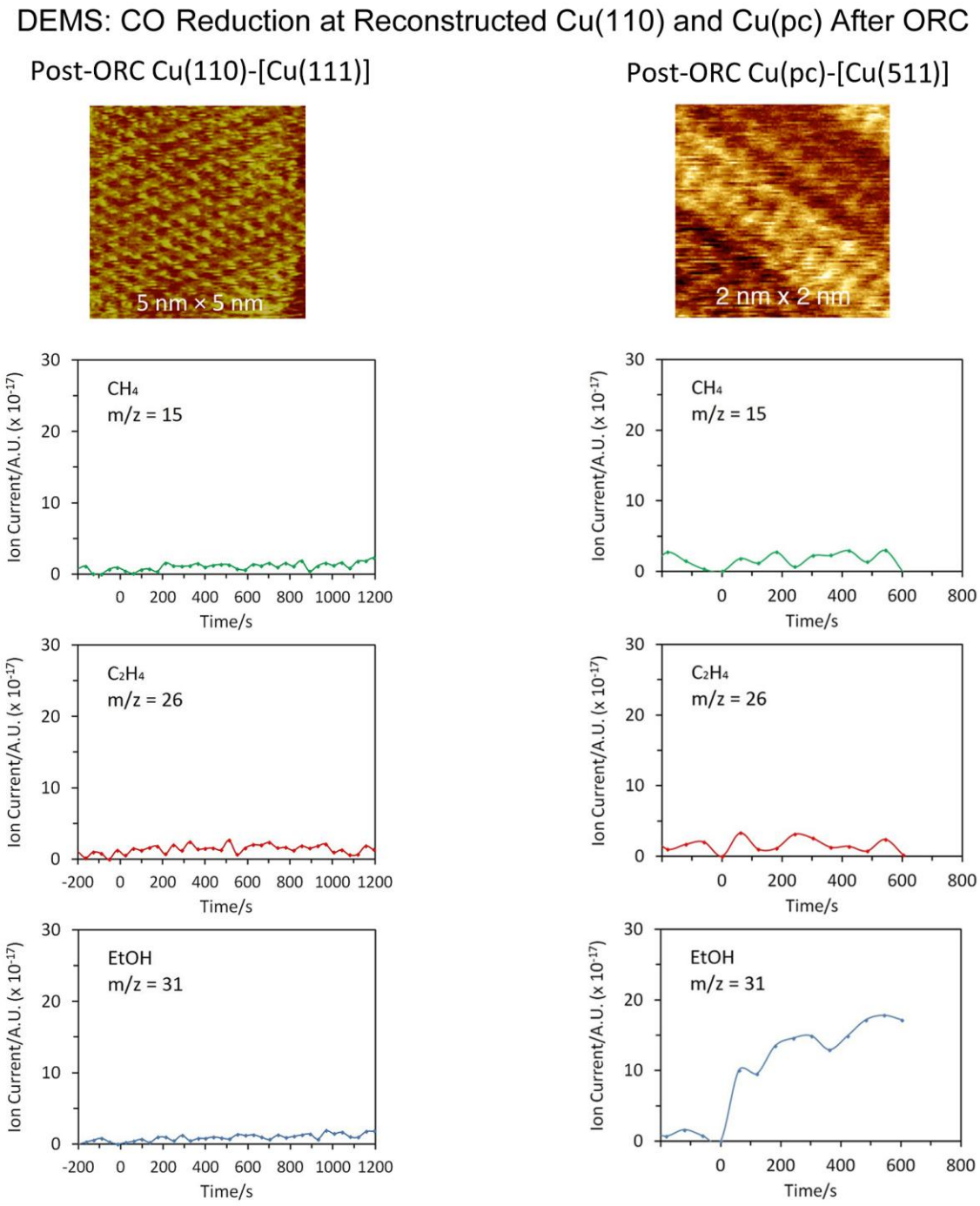

Figure 4. Plots of ion current as a function of time for CH_4 (m/z = 15), C_2H_4 (m/z = 26), and C_2H_5OH (m/z = 31) generated from the constant-potential cathodic electrolysis, at -1.06 V (SHE), of CO at post-ORC reconstructed Cu(110) and Cu(pc) in 0.1 *M* KOH solution saturated with carbon monoxide. Experimental details are as described in the text.

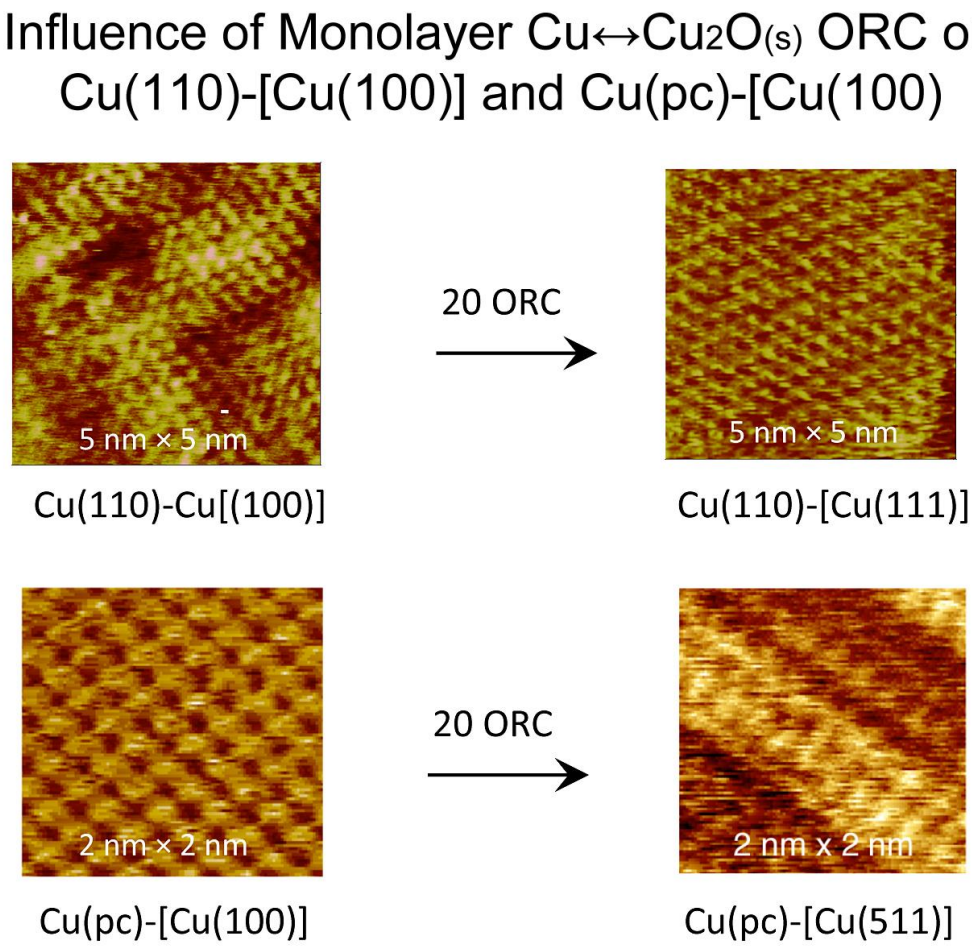

Figure 5. *Operando* ECSTM of the reconstructed Cu(pc)-[Cu(100)] and Cu(110)-[Cu(100)] surfaces before and after twenty $Cu_{(s)}\leftrightarrow Cu_2O_{(s)}$ oxidation-reduction cycles (ORC). In all cases, the potential was kept constant at -0.9 V (SHE) in 0.1 *M* KOH. Experimental details were as in Figure 1.

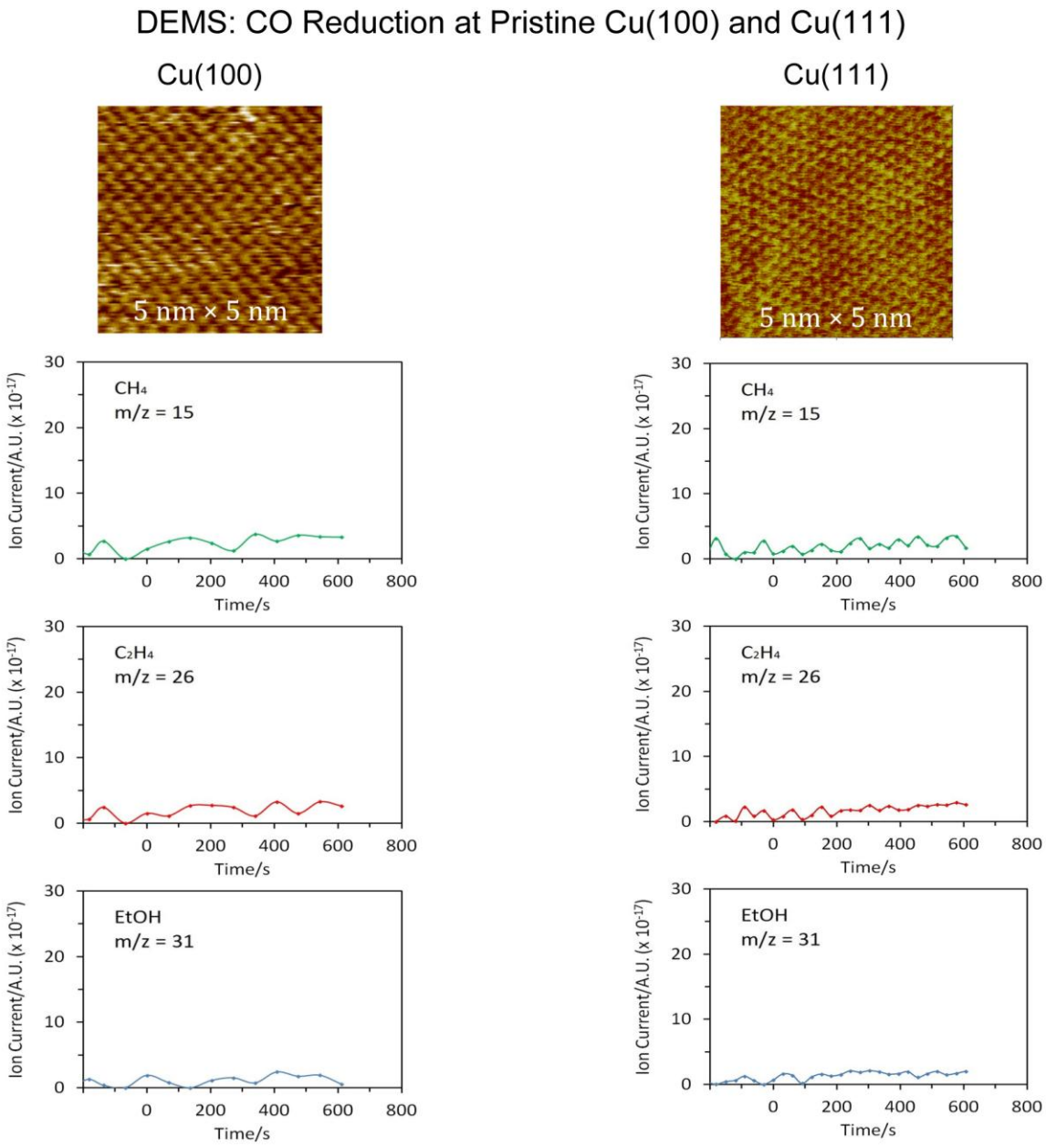

Figure 6. Plots of ion current as a function of time for CH_4 (m/z = 15), C_2H_4 (m/z = 26), and C_2H_5OH (m/z = 31) generated from the constant-potential cathodic electrolysis, at -1.06 V (SHE), of CO at pristine Cu(100) and Cu(111) in 0.1 *M* KOH solution saturated with carbon monoxide. Experimental details are as described in the text.